Flexibility and Cation Distribution upon Lithium Exchange of Aluminosilicate and Aluminogermanate Materials with the RHO Topology

Geoffrey M. Johnson,[†] Barbara A. Reisner,*[,†,||] Akhilesh Tripathi,[‡] David R. Corbin,[§] Brian H. Toby,[||] and John B. Parise[†,‡]

Department of Geosciences State University of New York, Stony Brook, New York 11794-2100, Department of Chemistry, State University of New York, Stony Brook, New York 11794-3400, Central Research and Development, DuPont Company, Inc., Experimental Station, P.O. Box 80262, Wilmington, Delaware 19880-0262, and Center for Neutron Research, National Institute of Standards and Technology, Gaithersburg, Maryland 20899-8562

Received March 26, 1999. Revised Manuscript Received July 12, 1999

The influence of lithium substitution on the structure of aluminosilicate (AlSi) and aluminogermanate (AlGe) materials with the zeolite RHO topology has been examined. The exchanged materials were dehydrated and structurally characterized via Rietveld refinement using neutron powder diffraction data. Li−AlSi-rho crystallizes in the space group $I\bar{4}3m$ with $a = 14.2609(3)$ Å, whereas Li−AlGe−rho adopts the space group $I23$ with $a = 14.2926(5)$ Å. The extraframework cations reside in their expected positions in Li−AlSi-rho: cesium is found in the double eight ring (D8R) and lithium is observed only in the single six ring (S6R). In Li−AlGe-rho, lithium resides in both the single six ring and the single eight rings (S8R) while cesium is located exclusively in the S6R. Although these cation positions are unusual for materials with the RHO topology, they are a response to the framework distortions introduced by ion exchange and dehydration. The extraframework cation positions correspond to those that best satisfy the coordination requirements of each cation.

Introduction

Ion exchange is one of the fundamental properties of zeolites, central to their importance as industrial materials.[1−4] This is exemplified by the widespread use of zeolite A as a detergent builder, in which calcium and magnesium ions are removed from washing water to prevent their precipitation by surfactant molecules.[5,6] Such commercial utility stems from the nontoxic nature of zeolites that degrade to soil-like materials. Exchange of the nonframework cations can be used to modify the characteristics of the zeolite: LTA is a well-known example for which the sodium, potassium, and calcium forms have effective apertures of approximately 4, 3, and 5 Å, respectively.[1,2] Such ion-exchange procedures allow for tailoring of effective pore apertures, which is crucial for selective gas separation and molecular-sieving ability.

The ion-exchange properties of aluminosilicate zeolites are governed in part by the framework Si/Al ratio: the number of monovalent cations required to charge balance the framework is equal to the aluminum content, since for each aluminum present there is a single net negative charge associated with the framework.[1−3] Modification of the framework components plays a significant role in tailoring the degree of the ion-exchange capacity of a zeolite. In conjunction with Loewenstein's rule of adjacent aluminum avoidance,[7] the maximum ion-exchange capacity is achieved for a framework silicon-to-aluminum ratio of unity. In addition to changing the ratio of framework species, modifications involving isomorphous substitution for aluminum and silicon can be performed, most commonly via alterations in the synthesis gel. Many elements have been introduced onto the framework sites of zeolites, including B, Ga, Ge, Cr, Mn, Fe, Zn, and Ti.[1,2] The different sizes and electronic configurations of the framework components directly influence the properties of the resulting material. For example, it is easy to envisage how inserting a tetrahedral element of differing size to Al or Si will change the pore sizes of a particular zeolite and hence the molecular-sieving characteristics. Since the extraframework cations coordinate to the oxygens in a zeolite framework, changing the size of the rings and channels may affect these interactions

* To whom correspondence should be addressed.
[†] Department of Geosciences, SUNY.
[‡] Department of Chemistry, SUNY.
[§] DuPont Company, Inc., publication no. 7922.
[||] National Institute of Standards and Technology.

(1) Breck, D. W. *Zeolite Molecular Sieves, Structure, Chemistry and Uses*; Wiley-Interscience: New York, 1974.
(2) Barrer, R. M. *Zeolites and Clay Minerals as Sorbents and Molecular Sieves*; Academic Press: London, 1978.
(3) Barrer, R. M. *Hydrothermal Chemistry of Zeolites*; Academic Press: London, 1982.
(4) Newsam, J. M. *Science* **1986**, *231*, 1093.
(5) Meier, W. M.; Olson, D. H.; Baerlocher, C. *Atlas of Zeolite Structure Types*, 4th ed.; Elsevier: London, 1996.
(6) Newsam, J. M.; Treacy, M. M. J. *Zeolites* **1993**, *13*, 183.
(7) Loewenstein, W. *Am. Miner.* **1954**, *39*, 92.

10.1021/cm990179g CCC: $18.00
Published on Web 09/16/1999

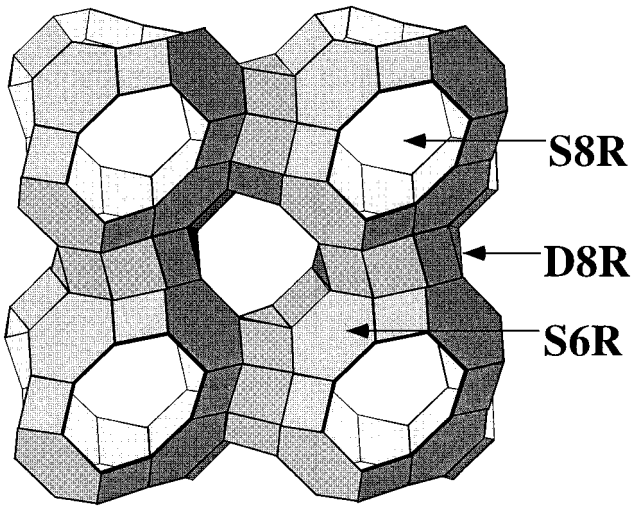

Figure 1. The RHO structure in space group $I\bar{4}3m$ showing the six rings and elliptical eight rings formed by linkage of T centers with oxygen atoms. The vertexes correspond to T atoms. Oxygen atoms have been excluded for clarity.

and perhaps the location of the cations occupying the intracrystalline voids. This, in turn, can modify the ion-exchange properties of the zeolite framework material.

In general, zeolites are considered to be rigid structures, with control of the pore size often achieved via variation in the nature and amount of extraframework cations as was described above for zeolite A.[5,6] In such cases, the change in aperture dimensions is not connected to a framework distortion, but is simply related to the relative degrees to which different-sized cations block the zeolite windows. In contrast, zeolite RHO (Figure 1) undergoes framework distortions upon alteration in the type of extraframework cation and degree of hydration.[5,6,8−26] This unusual flexibility has been extensively investigated for aluminosilicate compositions.[9−26] We recently reported the synthesis and characterization of an aluminogermanate with the zeolite RHO topology[27,28] that possesses a framework Ge/Al ratio of unity. This contrasts with aluminosilicate rho which tends to have Si/Al ∼ 3,[8,29,30] but is more similar to the gallosilicate which has Si/Ga ∼ 1.3.[31] The aluminogermanate is particularly interesting since it possesses the maximum ion-exchange capacity of a zeolite as well as the flexibility associated with frameworks with the RHO topology. This paper reports a comparison between the lithium-exchanged forms of aluminosilicate and aluminogermanate materials with the RHO topology, which reflects our ongoing interest in the structure/property relationships associated with substitution of both framework and nonframework cations in zeolites and related microporous crystalline molecular sieves.

Experimental Section

Sample Preparation. *Li−AlGe-rho.* Na,Cs−AlGe-rho was synthesized from a gel mixture with composition Cs_2O:Na_2O:GeO_2:Al_2O_3:H_2O/0.7:2.3:2:1:70 according to the procedure reported by Johnson and co-workers.[28] The synthesis yields a material with approximate composition $Na_{16}Cs_8Al_{24}Ge_{24}O_{96}$. Li−AlGe-rho was prepared by standard ion-exchange methods. A dried sample was exchanged by contacting the material five times (1 h/cycle) with 2 M aqueous LiCl (10 mL/g) solution at 60 °C. ICP chemical analysis (DuPont) gave a chemical composition of $Li_{13.9}Cs_{5.24}Na_{0.24}Al_{24.4}Ge_{23.6}O_{96}$.

Li−AlSi-rho. Na,Cs−AlSi-rho was prepared by a modification of the method first reported by Robson.[29] The NH_4−AlSi-rho was prepared using standard ion-exchange procedures. This was followed by Na^+ exchange by contacting the material six times (1 h/cycle) with a 10% w/w aqueous $NaNO_3$ (10 mg/L) solution at 90 °C to yield Na−AlSi-rho. The Na−AlSi-rho was then exchanged six times (1 h/cycle) with a 10% w/w aqueous $LiNO_3$ (10 mg/L) solution at 90 °C to yield Li−AlSi-rho. ICP chemical analysis (DuPont) gave a chemical composition of $Li_{7.6}Cs_{1.3}Na_{2.0}Al_{11.4}Si_{36.6}O_{96}$.

Powder Neutron Diffraction Data Collection. In preparation for the diffraction experiment, 2 g of the aluminogermanate and 1 g of the aluminosilicate were treated with three cycles of dehydration under vacuum at 300 °C and exposed to D_2O at 5 Torr on a vacuum rack. To avoid degradation of the materials, each cycle was conducted using a 16-h temperature ramp for heating and cooling. Following this treatment, the samples were sealed in Pyrex glass vials under vacuum at a pressure of less than 1 mTorr. Directly prior to data collection, the samples were transferred into and sealed within vanadium cans of 3/8-in. diameter in a helium environment with water levels <10 ppm.

Neutron powder diffraction data were collected on the High-Resolution Powder Diffractometer (BT-1) at the NIST Center for Neutron Research at the National Institute of Standards and Technology. Measurements were performed at ambient

(8) Robson, H. E.; Shoemaker, D. P.; Ogilvie, R. A.; Manor, P. C. *Molecular Sieves*; Meier, W. M., Uytterhoeven, J. B., Eds.; American Chemical Society: Washington, DC, 1973; p 106.
(9) Corbin, D. R.; Abrams, L.; Jones, G. A.; Eddy, M. M.; Stucky, G. D.; Cox, D. E. *J. Chem. Soc., Chem. Commun.* **1989**, 42.
(10) Corbin, D. R.; Stucky, G. D.; Eddy, M. M.; Prince, E.; Abrams, L.; Jones, G. A. *Abstracts of Papers, 193rd Meeting of the American Chemical Society, Denver, CO*; American Chemical Society: Washington, DC, 1987; INOR 300.
(11) Corbin, D. R.; Abrams, L.; Jones, G. A.; Eddy, M. M.; Harrison, W. T. A.; Stucky, G. D.; Cox, D. E. *J. Am. Chem. Soc.* **1990**, *112*, 4821.
(12) Parise, J. B.; Prince, E. *Mater. Res. Bull.* **1983**, *18*, 841.
(13) McCusker, L. B. *Zeolites* **1984**, *4*, 51.
(14) McCusker, L. B.; Baerlocher, C. In *Proceedings of the Sixth International Zeolite Conference*; Olson, D. H., Bisio, A., Eds.; Butterworth: Guildford, Surrey, 1984; p 812.
(15) Parise, J. B.; Abrams, L.; Gier, T. E.; Corbin, D. R.; Jorgensen, J. D.; Prince., E. *J. Phys. Chem.* **1984**, *88*, 2303.
(16) Parise, J. B.; Gier, T. E.; Corbin, D. R.; Cox, D. E. *J. Phys. Chem.* **1984**, *88*, 1635.
(17) Wright, P. A.; Thomas, J. M.; Ramdas, S.; Cheetham, A. K. *J. Chem. Soc., Chem. Commun.* **1984**, 1338.
(18) Fischer, R. X.; Baur, W. H.; Shannon, R. D.; Staley, R. H.; Vega, A. J.; Abrams, L.; Prince, E. *J. Phys. Chem.* **1986**, *90*, 4414.
(19) Baur, W. H.; Fischer, R. X.; Shannon, R. D.; Staley, R. H.; Vega, A. J.; Abrams, L.; Corbin, D. R.; Jorgensen, J. D. *Z. Kristallogr.* **1987**, *179*, 281.
(20) Fischer, R. X.; Baur, W. H.; Shannon, R. D.; Staley, R. H. *J. Phys. Chem.* **1987**, *91*, 2227.
(21) Fischer, R. X.; Baaur, W. H.; Shannon, R. D.; Staley, R. H.; Abrams, L.; Vega, A. J.; Jorgensen, J. D. *Acta Crystallogr.* **1988**, *B44*, 321.
(22) Gameson, I.; Rayment, T.; Thomas, J. M.; Wright, P. A. *J. Phys. Chem.* **1988**, *92*, 988.
(23) Baur, W. H.; Bieniok, A.; Shannon, R. D.; Prince, E. *Z. Kristallogr.* **1989**, *187*, 253.
(24) Fischer, R. X.; Baur, W. H.; Shannon, R. D.; Parise, J. B.; Faber, J.; Prince, E. *Acta Crystallogr.* **1989**, *C45*, 983.
(25) Corbin, D. R.; Abrams, L.; Jones, G. A.; Harlow, R. L.; Dunn, P. *Zeolites* **1991**, *11*, 364.
(26) Parise, J. B.; Xing, L.; Corbin, D. R. *J. Chem. Soc., Chem. Commun.* **1991**, 162.
(27) Johnson, G. M.; Tripathi, A.; Stephens, P. W.; Parise, J. B. Synthesis and Structure of an Aluminogerminate Zeolite with the RHO Topology, Recent Progress Report #27. Presented at the 12th International Zeolite Conference, Baltimore, MD, 1998.
(28) Johnson, G. M.; Tripathi, A.; Parise, J. B. *Micropor. Mesopor. Mater.* **1999**, *28*, 139.
(29) Robson, H. E. U.S. Patent 3,904, 753, 1975.
(30) Barrer, R. M.; Barri, S.; Klinowski, J. In *Proceedings of the Fifth International Zeolite Conference*; Rees, L. V. C., Ed.; Elsevier: Amsterdam, 1980; p 20.
(31) Newsam, J. M.; Vaughan, D. E. W.; Strohmaier, K. G. *J. Phys. Chem.* **1995**, *99*, 9924.

conditions using an incident wavelength of $\lambda = 2.0784$ Å, using a Ge(311) monochromator.

Results

Structure Refinement. *Li−AlGe-rho.* The starting model for Rietveld analysis was that of the as-synthesized Na,Cs−AlGe-rho material in space group *I*23.[28] This is consistent with a strictly ordered alternating arrangement of framework Al and Ge, for Ge/Al = 1 (chemical analysis yields Ge/Al = 0.97) as required by Loewenstein's rule[7] which is believed to extend to aluminogermanates.[28] The data were analyzed using the Rietveld technique[32,33] in conjunction with the GSAS (Generalized Structure Analysis System) suite of Larson and Von Dreele.[34] Initial refinement followed the procedure outlined for the parent Na,Cs−AlGe-rho.[28] Since chemical analysis indicated that only a small amount of sodium (approximately 0.2 Na^+ per unit cell) remained after lithium exchange, sodium was not included in the model. In Na,Cs−AlGe-rho, two distinct sites were used to account for each of the extraframework cations, with sodium in the S6R and S8R sites and cesium in the D8R and S6R sites. Chemical analysis indicated that lithium preferentially substitutes for sodium, and hence the initial model used here involved Li^+ on the previous Na^+ sites. Occupancies of the cesium sites were lowered to correspond to a reduction from 8 to 5.24 cesium cations per unit cell.

Following refinement of the framework species, the positions and occupancies of Li^+ and Cs^+ were examined. These cations are readily distinguished due to their markedly different neutron-scattering lengths and cation−oxygen bond lengths. Lithium cations were found in both S8R and S6R sites, the positions previously occupied by sodium in the Na,Cs−AlGe-rho parent. Refinement of the fractional occupancies indicated that the S6R and S8R sites were 84(8)% and 40(5)% occupied, respectively. This translates to a total lithium content of 16.3 per unit cell. Considering the weak scattering power of lithium, this is in reasonable agreement with the 13.9 Li^+ per unit cell obtained from chemical analysis.

When located in the D8R sites, Cs−O distances of approximately 2.66 Å were obtained, which is far shorter than the sum of their ionic radii, 3.04 Å.[35] Since this is chemically unreasonable, alternative sites for Cs^+ were examined. If cesium was located in the S8R, a Cs−O separation distance 12% shorter than that expected from a hard-spheres model would be obtained. Therefore, the S6R site was chosen. Subsequent refinement supported this model, and the fractional occupancy of Cs^+ converged to an occupancy of 68(3)%, corresponding to 5.44(2) Cs^+ per unit cell, in accordance with the ICP analysis.

Fourier difference analysis at this stage indicated that a small amount of residual scattering density was associated with the D8R site. The presence of a small amount of sodium in the D8R was examined, but long separation distances of 2.67 Å, coupled with a refined population of 2.3 Na^+ (0.2 Na^+ by ICP), indicated that this model was unrealistic. Since previous work indicated that only Cs^+, D_2O, and ND_4^+ have been observed in the D8R sites,[10,11,15,18,24,36−38] it seems likely that this scattering is associated with a small amount of D_2O remaining from sample preparation. The cation distribution in this material is discussed in more detail below.

During the final cycles of refinement, the weights of the soft constraints were reduced gradually to zero and a stable refinement still resulted. The data did not allow for the refinement of individual displacement parameters for all atoms, so isotropic atomic displacement parameters were grouped, using one value for framework T atoms, a second value for framework O atoms, and a third for extraframework cations. Atomic coordinates and refinement parameters are summarized in Table 1, with selected bond distances and angles given in Table 2. The final observed and calculated diffraction profiles are displayed in Figure 2.

Li−AlSi-rho. The diffraction data for Li−AlSi-rho were analyzed using the general procedure described above. Initial fractional atomic coordinates for the

Table 1. Final Atomic Parameters for Dehydrated Li−AlGe-rho Refinement Using Neutron Powder Diffraction Data with Standard Uncertainties in Parentheses[a]

atom	site	*x*	*y*	*z*	*B* (Å^2)	occ.
Al	24f	0.2874(15)	0.1335(16)	0.4379(14)	1.79(16)	1
Ge	24f	0.2124(7)	−0.0614(7)	0.3627(7)	1.79(16)	1
O(1)	24f	0.2504(8)	0.2479(8)	0.4107(5)	1.67(9)	1
O(2)	24f	0.4034(7)	0.1258(5)	0.4022(8)	1.67(9)	1
O(3)	24f	0.2856(10)	0.1139(9)	0.5570(8)	1.67(9)	1
O(4)	24f	0.2126(10)	0.0593(9)	0.3770(8)	1.67(9)	1
Cs(1)	8c	0.1786(13)	0.1786(13)	0.1786(13)	4.10(13)	0.68(3)
Li(1)	8c	0.3138(28)	0.3138(28)	0.3138(28)	4.10(13)	0.84(8)
Li(2)	24f	0.387(5)	−0.037(6)	−0.069(5)	4.10(13)	0.40(5)

[a] Space group: *I*23(197). Found: $Li_{16.32}Cs_{5.44}$ (by refinement). $a = 14.2926(5)$ Å; $\alpha = \beta = \gamma = 90°$. $\chi^2 = 0.813$. $R_{Bragg} = 4.10\%$; wRp = 6.06%; Rp = 4.95%.

Table 2. Selected Interatomic Distances and Angles Derived from Dehydrated Li−AlGe-rho Refinement with Standard Uncertainties in Parentheses

atoms	distance (Å)	atoms	angle (deg)
Al(1)−O(1)	1.762(21)	O(1)−Al−O(2)	106.3(13)
Al(1)−O(2)	1.738(21)	O(1)−Al−O(3)	111.4(13)
Al(1)−O(3)	1.724(19)	O(1)−Al−O(4)	105.7(12)
Al(1)−O(4)	1.741(21)	O(2)−Al−O(3)	107.1(13)
⟨Al(1)−O⟩	1.741	O(2)−Al−O(4)	113.6(13)
Ge(1)−O(1)	1.759(13)	O(3)−Al−O(4)	112.6(13)
Ge(1)−O(2)	1.722(14)	O(1)−Ge−O(2)	109.2(8)
Ge(1)−O(3)	1.725(13)	O(1)−Ge−O(3)	108.5(7)
Ge(1)−O(4)	1.737(13)	O(1)−Ge−O(4)	109.3(7)
⟨Ge(1)−O⟩	1.736	O(2)−Ge−O(3)	112.7(7)
		O(2)−Ge−O(4)	106.1(3)
Li(1)−O(1)	1.904(13)	O(3)−Ge−O(4)	110.8(3)
Li(2)−O(2)	1.98(8)	Al−O(1)−Ge	121.7(7)
Li(2)−O(3)	2.10(8)	Al−O(2)−Ge	121.9(3)
Cs−O(1)	3.611(28)	Al−O(3)−Ge	137.5(13)
Cs−O(3)	3.476(13)	Al−O(4)−Ge	131.7(11)
Cs−O(4)	3.344(17)	⟨Al−O−Ge⟩	128.2

(32) Rietveld, H. M. *J. Appl. Crystallogr.* **1969**, *2*, 65.
(33) Young, R. A. *The Rietveld Method: IUCr Monographs on Crystallography*; Oxford University Press: New York, 1993.
(34) Larson, A. C.; VonDreele, R. B. *GSAS: General Structure Analysis System Manual*; Los Alamos Report LAUR 86-748; Los Alamos National Laboratory: Los Alamos, NM, 1986.
(35) Shannon, R. D.; Prewitt, C. T. *Acta Crystallogr.* **1976**, *A32*, 751.
(36) Mortier, W. J. *Compilation of Extra Framework Sites in Zeolites*; Butterworth: Surrey, U.K., 1982.
(37) Stucky, G. D.; Eddy, M. M.; Corbin, D. R.; Abrams, L.; Jones, G. A.; Prince, E. Presented at the American Crystallographic Association Meeting, McMaster University, Ontario, Canada, June 1986.
(38) Baur, W. H.; Fischer, R. X.; Shannon, R. D. In *Innovation in Zeolite Materials Science*; Grobet, P. J., Mortier, W. J., Vansant, E. F., Schultz-Ekloff, G., Eds.; Elsevier: Amsterdam, 1988; p 281.

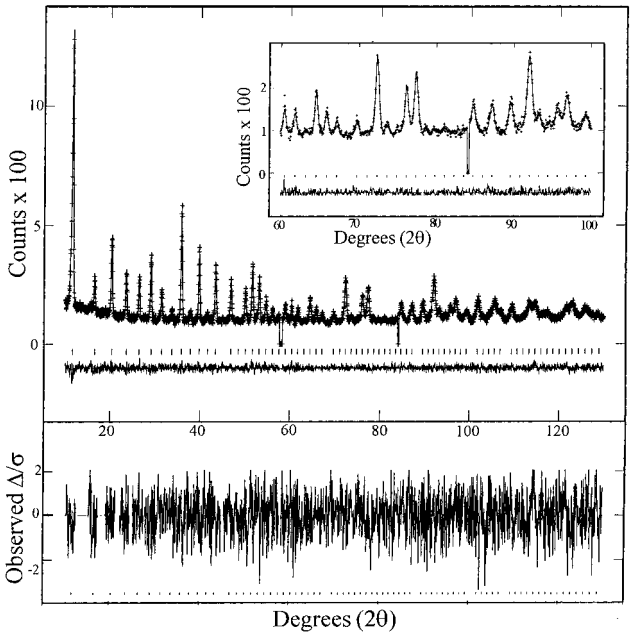

Figure 2. Results of Rietveld refinement of the structure of dehydrated lithium aluminogermanate rho using neutron powder diffraction data at room temperature. The tic marks indicate the positions of reflections, and the difference curve is shown at the bottom on the same scale. The region 60° < 2θ < 100° is magnified in the upper right. The lower box shows the deviations relative to the standard uncertainties for each point.

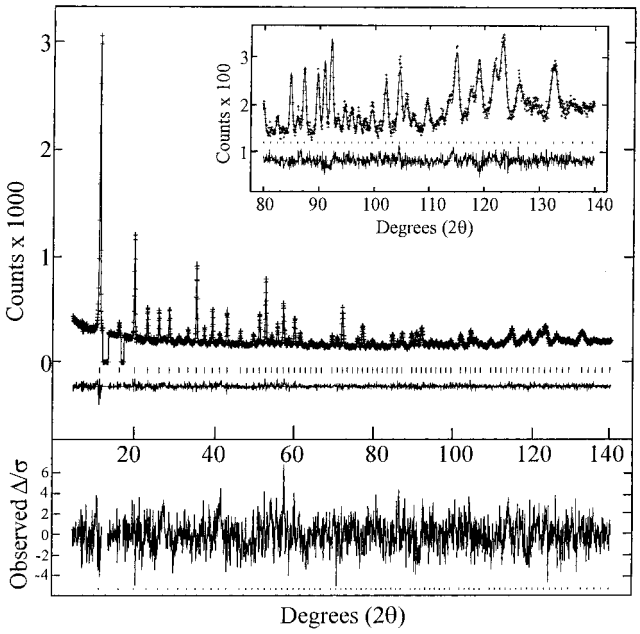

Figure 3. Results of Rietveld refinement of the structure of dehydrated lithium aluminosilicate rho using neutron powder diffraction data at room temperature. The tic marks indicate the positions of reflections, and the difference curve is shown at the bottom on the same scale. The region 80° < 2θ < 140° is magnified in the upper right. The lower box shows the deviations relative to the standard uncertainties for each point.

framework constituents in space group $I\bar{4}3m$ were based upon prior investigations of this material.[10,37] Aluminum and silicon were modeled using a single T site, with the fractional occupancies fixed in accordance with chemical analysis to account for the difference in scattering between aluminum and silicon. Throughout the refinement, their positions and thermal parameters were constrained to be identical. Two separate sites were used to account for the extraframework cations; Li^+ was situated on the S6R site ($x = y = z$) while Cs^+ was placed at the center of the D8R (1/2,0,0). The fractional occupancies of the extraframework cations, 95% for Li^+ and 22% for Cs^+, were initially fixed to correspond to the values obtained from elemental analysis. At this stage, a difference plot between the calculated and observed data indicated the presence of a crystalline impurity phase, most clearly seen at 2θ (deg) values of 12.5, 12.9, 13.8, 17.5, 27.8, and 44.1. The most intense impurity peaks, in the region of 13° and at 17°, did not overlap with the RHO peaks and were excluded in the refinement. The other impurity peaks remained in the refinement and are clearly visible through examination of the difference plots (Figure 3).

Upon refinement, the extraframework cations did not move appreciably from their starting positions. The calculated Cs−O (2.97 Å) and Li−O (1.96 Å) bond distances are in good agreement with the values expected from the sum of their ionic radii, 3.04 and 1.94 Å, respectively.[35] At this stage, various sites for Na^+ were examined, including the S8R and S6R sites, but neither of these models yielded stable refinements. Fourier difference analysis at this stage indicated residual scattering density skewed toward the S8R in the D8R. Subsequent positional refinements of Na^+ on this site converged. The calculated Na−O(3) bond length of 2.51(4) Å matches that for Na(2)−O(3) observed by Newsam et al. for ECR-10, a gallosilicate with the RHO topology.[31] Calculation of the bond valence parameter for this sodium yields a value of 59.4%, which is rather low compared with the expected value of unity.[39] A separate refinement in which this scattering was attributed to D_2O did not significantly influence any other structural parameters in the material, and in fact yielded a slightly poorer fit to the data. Therefore, to account for this scattering, it was deemed to be most appropriate to retain sodium in this eight-ring position.

After positional refinements were stable, fractional occupancies of the extraframework cations were permitted to vary. The resulting fractional occupancies were 84(4)% for Li^+, 20(2)% for Cs^+, and 16(2)% for Na^+. This translates to $6.7Li^+$ per unit cell, $1.2Cs^+$ per unit cell, and $3.8Na^+$ per unit cell. The values obtained for Li^+ and Cs^+ are in good agreement with chemical analysis.

During the final cycles of the refinement the soft constraints were removed and a stable refinement persisted. Isotropic atomic displacement parameters were grouped, using one value for framework T atoms, a second value for framework O atoms and a third for extraframework cations. Atomic coordinates and refinement parameters are summarized in Table 3, with selected bond distances and angles given in Table 4. The final observed and calculated diffraction profile are displayed in Figure 3.

Discussion

Mechanisms of Cell Contraction of RHO upon Lithium Exchange. The introduction of lithium cations into aluminosilicate and aluminogermanate rho

(39) Brown, I. D.; Altermatt, D. *Acta Crystallogr.* **1985**, *B41*, 244.

Table 3. Final Atomic Parameters for Dehydrated Li−AlSi-rho Refinement Using Neutron Data with Standard Uncertainties in Parentheses[a]

atom	site	*x*	*y*	*z*	*B* (Å^2)	occ.
Al	48h	0.2776(3)	0.1277(4)	0.4273(3)	1.3(1)	0.762
Si	48h	0.2776(3)	0.1277(4)	0.4273(3)	1.3(1)	0.238
O(1)	24g	0.2289(3)	0.2289(3)	0.3965(5)	2.34(7)	1
O(2)	24 g	0.1164(2)	0.1164(2)	0.6274(4)	2.34(7)	1
O(3)	48h	0.0410(2)	0.2143(3)	0.3834(3)	2.34(7)	1
Li	8c	0.2932(16)	0.2932(16)	0.2932(16)	2.5	0.84(4)
Cs	6b	0.5	0	0	2.5	0.20(2)
Na	24 g	0.046(3)	0.434(4)	0.046(3)	2.5	0.16(2)

[a] Space group: $I\bar{4}3m$(217). Found: $Li_{6.7}Na_{3.8}Cs_{1.2}$ (by refinement). a = 14.2609(3) Å; $\alpha = \beta = \gamma = 90°$. χ^2 = 1.972. R_{Bragg} = 5.55%; wRp = 5.06%; Rp = 4.09%.

Table 4. Selected Interatomic Distances and Angles for Dehydrated Li−AlSi-rho with Standard Uncertainties in Parentheses

atoms	distance (Å)	atoms	angle (deg)
T−O(1)	1.661(6)	O(1)−T−O(2)	106.8(4)
T−O(2)	1.634(5)	O(2)−T−O(3)	111.0(4)
T−O(3)	1.654(6)	O(2)−T−O(3)	108.3(4)
T−O(3)	1.633(6)	O(1)−T−O(3)	108.68(31)
⟨T−O⟩	1.646	O(1)−T−O(3)	112.1(4)
Li−O(1)	1.963(9)	O(3)−T−O(3)	110.0(4)
Na−O(2)	2.675(30)	T−O(1)−T	131.1(6)
Na−O(3)	2.51 (4)	T−O(2)−T	134.9(5)
Cs−O(2)	2.969(6)	T−O(3)−T	137.8(4)
Cs−O(3)	3.528(4)	⟨T−O−T⟩	134.6

materials causes significant unit cell contraction. Dehydrated Li−AlSi-rho has a cell parameter of 14.2609-(3) Å, while the dehydrated and hydrated, partially sodium-exchanged $Na_{9.97}Cs_{2.09}$−AlSi-rho of McCusker et al. have cell constants of 14.678 and 15.031(1) Å, respectively.[14] Hydrated Na,Cs−AlGe-rho has a cell parameter of 15.05(4) Å, compared with 14.6738(2) Å for the dehydrated Na,Cs−AlGe-rho[28] and 14.2926(5) Å for Li−AlGe-rho. This corresponds to a contraction in the unit cell volume upon lithium exchange of approximately 8.3% for the aluminosilicate and 7.6% for the aluminogermanate.

The mechanism of framework contraction in materials with the RHO topology is not simply confined to a reduction in the T−O−T angle. To maintain chemically reasonable framework T−O bond distances, there are concerted distortions of the ring systems (S6R and D8R) comprised of the smaller TO_4 tetrahedral units. Previous studies have described these distortions in terms of the deformation of the eight ring. A distortion parameter (Δ), defined as one-half of the difference between the major (long) and minor (short) axes of the S8R ellipse, was introduced to quantify the distortion.[12,15] A modified distortion parameter (Δ/a) was subsequently employed to account for variations in the bond lengths of the framework T−O bonds.[25] The ellipticity parameter (ζ), a third descriptor which is independent of the mean T−O distance, is defined as the ratio of the x-coordinates of oxygen atoms O(2) and O(3).[38] Geometrically, ζ is the ratio of the lengths of the major and minor axes of the S8R. The first parameter, Δ, is used in the following discussion since it best describes the deviation of the eight ring from circular (Δ = 0; $(d_{\text{major axis}})/(d_{\text{minor axis}}) = 1$) to elliptical geometry (Δ > 0; $(d_{\text{major axis}})/(d_{\text{minor axis}}) > 1$). Figure 4 compares the ellipticity of the S8R of aluminosilicate and aluminogermanate rho materials.

To maintain chemically reasonable T−O bond lengths, the TO_4 tetrahedra comprising the rho framework rotate

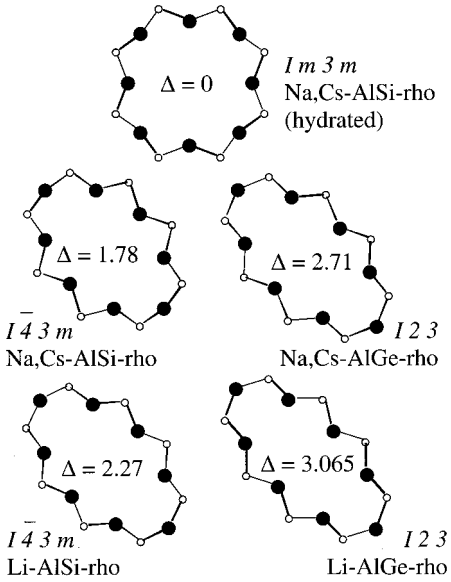

Figure 4. Comparison of eight-ring configurations and distortion parameters, Δ, for aluminosilicate and aluminogermanate rho materials.

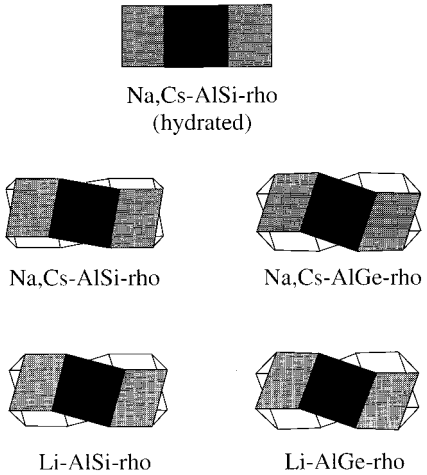

Figure 5. Projections of the eight rings along the (100) direction for a series of aluminosilicate and aluminogermanate rho materials, illustrating the eight-ring twisting that accompanies cell contraction.

as complete rigid units, known as rigid unit modes (RUMs).[40,41] In materials with the RHO topology, these concerted TO_4 motions occur in both the eight-ring and six-ring framework units. Figure 5 illustrates the twisting of the double eight rings that accompany the elliptical distortion of the single eight ring. Upon distortion of the single eight ring, the D8R twist from the planar geometry observed in circular (Δ = 0) hydrated Na,Cs−AlSi-rho. In these materials, the extent of the twist in the D8R appears to be directly related to the degree of elliptical distortion in the S8R. To our knowledge, Li−AlGe-rho exhibits the largest value of Δ observed for any material possessing the RHO topology, and hence displays the greatest elliptical distortion and twisting of the D8R.

A related distortion is observed in the configuration of the tetrahedral units comprising the six rings. While

(40) Dove, M. T.; Giddy, A. P.; Heine, V. In *Transactions of the American Crystallographic Association*; Wright, A. C., Ed.; American Crystallographic Association: Buffalo, NY, 1991; Vol. 27.

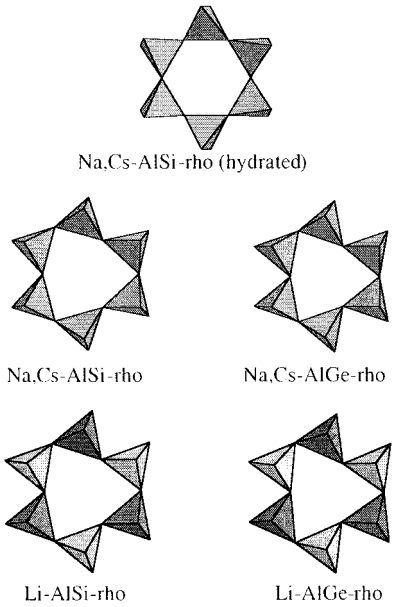

Figure 6. Projection of the six-ring windows for aluminosilicate and aluminogermanate rho materials along (111), indicating that the distortion of the six rings is a function of the unit cell composition.

the six ring in hydrated Na,Cs−AlSi-rho resembles a regular hexagon, it becomes more distorted as the level of cell contraction increases, reaching a maximum for the Li−AlGe-rho, as illustrated in Figure 6. Unlike the twist of the D8R, this trend appears to correlate with the cell parameter rather than with deformation of the S8R. This phenomenon strongly resembles a trend that is observed in materials with the sodalite structure, for which cell collapse is principally accommodated by cooperative rotations of TO_4 tetrahedra about their 4 axis.[42−46] We are currently investigating the mechanisms of cell contraction in the rho structure as a function of cation exchange to establish whether it can be described by a twist parameter similar to that used for the simpler sodalite system.

Nonframework Cation Distribution. The sites and occupancies of extraframework cations in the RHO framework materials have been the subject of extensive research and have previously been tabulated.[36] In the partially sodium-exchanged Na,Cs−aluminosilicate-rho with an extraframework cation content of $Na_{9.97}Cs_{2.09}$, McCusker and Baerlocher reported cesium in the D8R at (1/2,0,0), with approximately two-thirds of the sodium in the S8R and the remaining third in the S6R sites.[14] In the case of dehydrated Na,Cs−AlGe-rho, $Na_{16}Cs_8Al_{24}Ge_{24}O_{96}$, the cation distribution is markedly different from its aluminosilicate counterpart, predominantly due to the fact that the higher aluminum content requires a greater number of charge-balancing cations.[28] The 8c S6R site at ($x = y = z$) with $x \approx 0.3$ is fully occupied and the remainder of the sodium cations are located in the S8R site. Cesium cations occupy both the S6R and D8R sites with approximately 67% and 43% occupancies, respectively.

Table 5. Comparison of Extraframework Cation Sitings for Dehydrated Aluminosilicate and Aluminogermanate Materials with the RHO Topology

site	Na,Cs−AlSi[e]	Li−AlSi	Na,Cs−AlGe[e]	Li−AlGe
D8R[a]	Cs, 48%[f]	Cs, 20%	Cs, 43%	
S8R[b]	Na, 26%	Na, 16%	Na, 29%	Li, 40%
S6R[c]			Cs, 67%	Cs, 68%
S6R[d]	Na, 41%	Li, 84%	Na, 100%	Li, 84%
reference	14	*g*	28	*g*

[a] (0.5,0,0). [b] (x, y, z) where $x \approx 0.4$, $y \approx -0.05$, and $z \approx 0.05$. [c] ($x = y = z \approx 0.2$). [d] ($x = y = z \approx 0.3$). [e] The aluminosilicate rho listed above is a partially sodium-exchanged material while the aluminogerminate rho is an "as-synthesized" material. [f] Approximate percentage occupancy of site by the given cation. [g] This work.

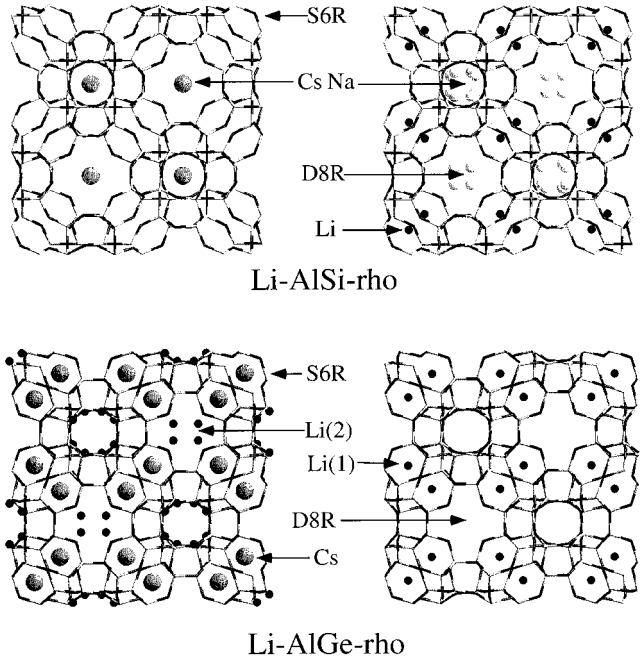

Figure 7. The structures of the dehydrated lithium-exchanged aluminosilicate and aluminogermanate rho materials showing the positions of the extraframework cations.

Lithium aluminosilicate rho is typical of materials with the RHO topology since its extraframework cation positions are similar to those observed in the parent material: cesium cations reside in the D8R position, lithium cations in the S6R, and sodium cations in the S8R. By contrast, lithium aluminogermanate rho is unusual since no cesium cations are found in the D8R, but instead are located only in the 8c ($x = y = z$) single six ring site. The lithium cations are distributed between the S8R and S6R sites. The positions and occupancies of the extraframework cations are summarized in Table 5, along with those for the Na,Cs−AlSi- and Na,Cs−AlGe-rho materials which are included for comparison.[14,28] Figure 7 provides a comparison of the extraframework cation positions in Li−AlSi- and Li−AlGe-rho.

These site preferences can be explained by several factors including the number of extraframework cations required for charge balance and the effect of cell contraction. The latter effect not only causes a distortion of the single six rings and double eight rings but also changes the size of the extraframework cation sites in

(41) Bieniok, A.; Hammonds, K. D. *Micropor. Mesopor. Mater.* **1998**, *25*, 193.
(42) Taylor, D.; Henderson, C. M. B. *Phys. Chem. Miner.* **1978**, *2*, 325.
(43) Dempsey, M. J.; Taylor, D. *Phys. Chem. Miner.* **1980**, *6*, 197.
(44) Depmeier, W. *Acta Crystallogr.* **1984**, *B40*, 185.
(45) Beagley, B.; Titiloye, J. L. *Struct. Chem.* **1992**, *3*, 429.
(46) Johnson, G. M.; Weller, M. T. *Stud. Surf. Sci. Catal.* **1997**, *105A*, 269.

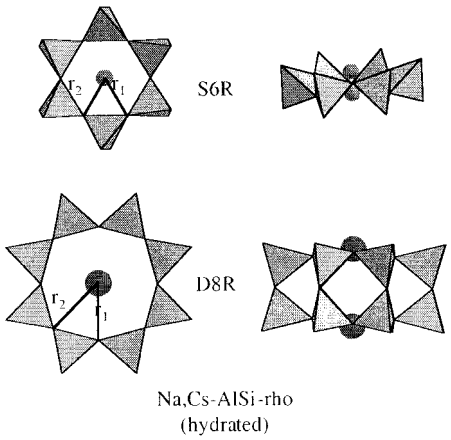

Figure 8. Extraframework cation positions in relation to the S6R and D8R for hydrated Na,Cs−AlSi-rho. Na^+ ions are represented as small gray spheres while Cs^+ ions are shown as large black spheres.

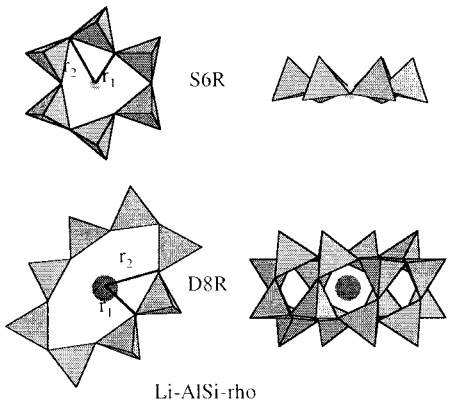

Figure 9. Extraframework cation positions in relation to the S6R and D8R for dehydrated Li−AlSi-rho. Li^+ ions are represented as small black spheres while Cs^+ ions are shown as large black spheres.

rho. Hydrated Na,Cs−AlSi-rho (*Im*3*m*) is the prototypical example of a RHO framework where there are no deviations of the S6R and D8R from their idealized "circular" geometries, as shown in Figure 8.[14] In hydrated Na,Cs−AlSi-rho, a mirror plane passes perpendicular to the C_6 axis so that there are equivalent Na^+ sites both above and below the S6R. In the undistorted single six ring, Na^+ has three strong Na−O bonding interactions (r_1 = 2.47 Å) and three weaker Na−O bonding interactions (r_2 = 2.72 Å). The double eight ring in Na,Cs−AlSi-rho is effectively planar and Cs^+ is comfortably sandwiched in the eight ring with four weak Cs−O bonding interactions (r_1 = 3.63 Å). The other oxygens in the D8R are sufficiently distant from Cs^+ that these interactions can be considered nonbonding (r_2 = 4.05 Å).

The amount of distortion observed in the S6R and D8R increases upon dehydration and lithium exchange of aluminosilicate rho, as is shown in Figure 9. The decrease in the cell length is accompanied by a distortion of the D8R away from planarity and the rotation of the tetrahedra comprising the S6R toward the C_3 rotation axis perpendicular to the plane of the ring. Similar to undistorted rho, Li−AlSi-rho has a single S6R site capable of three strong Li−O bonding interactions (r_1 = 1.96 Å). The Li−O distances are sufficiently long that Li^+ does not interact with the other oxygen located

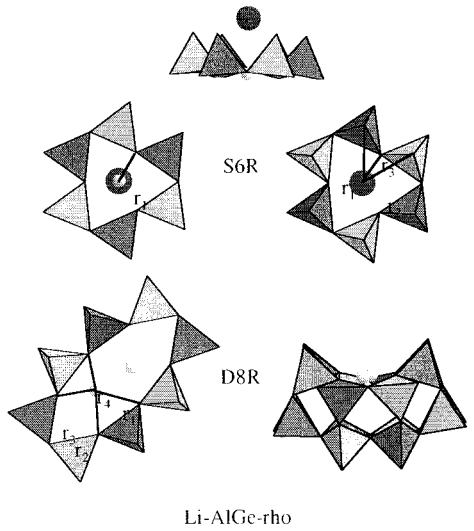

Figure 10. Extraframework cation locations in relation to S6R and D8R for dehydrated Li−AlGe-rho. Li^+ ions are represented as small gray spheres while Cs^+ ions are shown as large black spheres. $[GeO_4]^{4-}$ tetrahedra are shaded in dark gray and $[AlO_4]^{5-}$ tetrahedra are light gray in color.

in the plane of the S6R (r_2 = 2.97 Å). The eight ring is distorted and the D8R oxygen closest to the elliptical minor axis helps to create a smaller site for Cs^+ than what is observed in either of the Na,Cs−AlSi-rho sites. There are four strong Cs−O bonding interactions (r_1 = 2.97 Å) and eight weak Cs−O bonding interactions (r_2 = 3.53 Å). Although the framework is distorted from the idealized geometry of the hydrated Na,Cs−AlSi-rho, the positions of the extraframework cations in Li−AlSi-rho are very similar to those observed in the undistorted framework.[14]

The magnitude of the distortions in Li−AlGe-rho have a significant influence on the position of the extraframework cations. The rotation of TO_4 tetrahedra of the S6R is even more pronounced than that for Li−AlSi-rho, and hence they are even further rotated from the S6R plane toward the C_3 rotation axis such that the tetrahedra are nearly parallel to this axis. Although the extraframework cation site located near the plane of the S6R still exists, the rotation of TO_4 tetrahedra creates a second 24f S6R site, as seen in Figure 10. This apical site is occupied by Cs^+ and moderately strong Cs−O bonding interactions that arise from interactions with the apical oxygen of the S6R tetrahedra (r_1 = 3.33 Å; r_2 = 3.35 Å). The basal S6R site is occupied by Li^+ and provides an excellent coordination environment for Li^+ with three Li−O bonding interactions with r_1 = 1.91 Å.

The D8R in Li−AlGe-rho are distorted to such an extent that the size of the extraframework cation site at the center of the D8R has been significantly reduced. In this highly distorted state, the D8R site is so small that it can no longer accommodate Cs^+ between the two, connected S8R. Although the eight ring can no longer provide a suitable coordination environment for Cs^+, the large elliptical distortion creates sites that fulfill the coordination requirements of the small lithium cation. As depicted in Figure 10, there are two symmetry-related sites for lithium within each S8R. In the S8R,

Table 6. Comparison of Extraframework Cation−Oxygen Bond Lengths for Dehydrated Aluminosilicate and Aluminogermanate Rho Materials

	8R sites			6R sites		
RHO analog	Cs−O (Å)	Na−O (Å)	Li−O (Å)	Cs−O (Å)	Na−O (Å)	Li−O (Å)
Na,Cs−AlSi	3.08 (4×) 3.45 (4×)	2.74 (2×)			2.27 (3×)	
Li−AlSi	2.97 (4×) 3.53 (8×)	2.51 (2×) 2.67 (2×)				1.96 (3×)
Na,Cs−AlGe	2.92 (4×) 3.59 (4×) 3.63 (4×)	2.34 (1×) 2.39 (1×) 2.42 (1×) 2.54 (1×)		3.48 (3×) 3.54 (3×)	2.24 (3×)	
Li−AlGe			2.09 (1×) 2.10(1×) 2.41 (1×) 2.49 (1×)	3.33 (3×) 3.46 (3×) 3.59 (3×)		1.91 (3×)

each Li^+ has four Li−O interactions (r_1 = 2.09 Å; r_2 = 2.10 Å; r_3 = 2.41 Å; r_4 = 2.49 Å), with the strongest Li−O interactions (r_1 and r_2) occurring between Li^+ and the oxygen that are coordinated to the framework Al^{3+}.

While the positions of the extraframework cations in Li−AlGe-rho are unusual, closer inspection of the effective size of the extraframework sites upon ion-exchange-induced framework distortion shows that these "unusual" positions are just the chemically reasonable sites for the particular cations which reside there (Table 6). In dehydrated Na,Cs−AlSi-rho, the framework is somewhat distorted, but this distortion serves to satisfy the coordination requirements of Na^+ and Cs^+ once the waters of hydration are removed. Lithium exchange of this material produces a more distorted framework which causes further shrinkage of the unit cell. While there is contraction of the D8R, the D8R still provides a site of suitable size for Na^+ while the compression of the basal site in the S6R yields a better bonding environment for Li^+.

To maintain charge balance in aluminogermanate rho, both S6R sites must be occupied and Cs^+ is the only cation of sufficient size for its coordination requirements to be fulfilled in the apical S6R site. The cation distribution in this material (Table 5) can be explained using a model which accounts for both the number of extraframework cation sites and the size of these sites. While the basal S6R site in Na,Cs−AlGe-rho is fully occupied by Na^+, not all of the sodium cations required to maintain charge balance can be accommodated by the S6R; the remainder are coordinated in the S8R site. The cesium occupancy of the D8R is limited by the number of Na^+ in the S8R since the S8R and D8R are occupied in a mutually exclusive fashion.[28] Therefore the remaining cesium cations are coordinated by the apical oxygen of the S6R, the only other site which is capable of coordinating Cs^+. Similar trends are observed in Li−AlGe-rho. Like Na^+, lithium cations require a small site to satisfy their coordination requirements. They can exchange only into sites which satisfy their bonding requirements, such as the basal S6R and S8R sites. Li^+ cannot exchange with Cs^+ in the apical S6R site and thus the Cs^+ occupancy of this site remains constant throughout the exchange process.

Conclusions

Cation substitution in zeolite RHO has been further examined by incorporation of lithium into aluminosilicate and aluminogermanate materials. Lithium substitution and dehydration causes significant cell contraction, which is accompanied by large distortions of both the six and eight rings. The magnitude of the distortions in the ring systems is affected by the degree of hydration and by the size of the extraframework cations. Since the positions of the extraframework cations are partially dictated by the number needed to maintain charge balance, these cations adopt positions which best satisfy their own coordination requirements. In each of the dehydrated materials investigated in this study, the extraframework cations occupy the sites which provide the best extraframework cation−framework oxygen bonding interactions.

Acknowledgment. This work was supported by the National Science Foundation Grant DMR-9713375. We thank the DuPont Company for performing the ICP analysis. Penrose Hollins is acknowledged for his technical assistance. Certain trade names and company products are identified to adequately specify experimental procedures. Such identification does not imply recommendation or endorsement by the National Institute of Standards and Technology, nor does it imply that the products are necessarily the best available for the purpose.

CM990179G